

PACS numbers: 42.55.Wd; 42.60.By; 42.65.–k; 42.81.–i
DOI: 10.1070/QE2015v045n05ABEH015756

Conversion of ultrashort laser pulses to wavelengths above 3 μm in tapered germanate fibres

E.A. Anashkina, A.V. Andrianov, A.V. Kim

Abstract. **Tapered germanate fibres are proposed for effective adiabatic conversion of Raman soliton pulses to the mid-IR region. A theoretical analysis demonstrates that, in fibres with anomalous group velocity dispersion decreasing along their length, wavelengths of up to 3.5 μm can be reached, which are unattainable in fibres with a constant core diameter at the same parameters of a 2-μm input signal. The analysis relies on a one-way wave equation that takes into account the combined effect of dispersion, Kerr and Raman nonlinearities, nonlinear dispersion and optical losses and the frequency dependence of the effective fundamental transverse mode size.**

Keywords: *optical solitons, germanate fibres, tapered fibres with varying dispersion, DDF, Raman shift of the soliton pulse frequency, mid-IR region.*

1. Introduction

To date, tremendous progress has been made in the development of near-IR laser sources, including systems generating ultrashort pulses. At the same time, in the mid-IR region such sources are difficult to create for many reasons, in particular for lack of a wide class of gain media with appropriate parameters. Because of this, a promising approach is to convert pulses from the near-IR, a well-mastered spectral region, to the mid-IR by nonlinear optical techniques in crystals [1], gases, gas-filled capillary tubes [2] and optical fibres of specific chemical composition [3]. Even though solid-state laser systems lead the way in energy parameters, fibre laser sources can be used in many applications because they offer the advantages of compact design, relatively low cost, stability, high output beam quality and not requiring adjustments.

A rather important area of research is supercontinuum generation in the mid-IR region in chalcogenide, tellurite and fluoride glasses [4]. In addition, it has been shown in a recent theoretical study that, in a short piece of microstructured silica-based fibre, ultrashort pulses of light at 1.55 and 2 μm can be converted to wavelengths above 3 μm [5]. At the same time, ultrashort pulses in the range 2–3 μm and, according to numerical estimates, above 3 μm can be obtained using germanate fibres, which are easier to fabricate and enable one to produce an all-fibre laser system because they are similar in physical properties to silica fibres and can be fusion spliced by standard techniques. In particular, germanate fibres have been demonstrated to generate supercontinuum in the ranges 1.5–2.7 [6] and 1–2.6 μm [7] under pumping with an erbium-doped fibre laser, in the range 2–2.6 μm when pumped by a Cr:ZnS solid-state laser and in the range 1.9–3 μm using a thulium fibre laser as a pump source [8, 9]. Also, the possibility of producing frequency-tunable Raman solitons in the range 2–3 μm was examined in Ref. [10]. However, to our knowledge there have been no reports on light generation in germanate fibres at wavelengths above 3 μm.

In this paper, we present a theoretical analysis of the possibility of converting ultrashort pulses to wavelengths above 3 μm in germanate fibres with group velocity dispersion varying along their length, namely, the Raman conversion of the optical soliton frequency in optical fibres with anomalous dispersion decreasing along their length. In the literature, such fibres are referred to as dispersion decreasing fibres (DDFs). Note that dispersion management in optical fibres, including DDFs, allows one to convert soliton pulses in a wide range of parameters [11–20]. DDFs may have the form of tapered fibres (with a varying core diameter), because there is not only material dispersion but also waveguide dispersion, which depends on fibre diameter [21]. As shown by Andrianov et al. [19, 20], both theoretically and experimentally, the carrier wavelength of Raman solitons can be tuned from 1.5 to 2 μm in silica DDFs. The optical range reached to date can be extended by using pulses of a thulium-doped all-fibre laser system at a wavelength of 2 μm as input light and germanate DDFs, offering higher Kerr and Raman nonlinearities and lower optical loss, as a nonlinear Raman-active medium.

2. Analysis of pulse propagation in germanate fibres

The nonlinear dynamics of ultrashort pulses in optical fibres are often analysed in terms of a generalised nonlinear Schrödinger equation, which allows one to take into account an arbitrary dispersion profile, Kerr and Raman nonlinearities, nonlinear dispersion and optical losses [22]. At the same time, in the case of ultrabroadband conversion of optical pulses, it is important to include the frequency dependence of the effective fundamental transverse mode size (and hence that of the nonlinearity coefficient). We use a model based on the one-way wave equation [23]. The model allows one to take

E.A. Anashkina, A.V. Andrianov, A.V. Kim Institute of Applied Physics, Russian Academy of Sciences, ul. Ul'yanova 46, 603950 Nizhnii Novgorod, Russia; N.I. Lobachevsky State University of Nizhnii Novgorod, prosp. Gagarina 23, 603950 Nizhnii Novgorod, Russia; e-mail: elena.anashkina@gmail.com

Received 29 January 2015; revision received 6 February 2015
Kvantovaya Elektronika **45** (5) 437–442 (2015)
Translated by O.M. Tsarev

into account all the above-mentioned effects in tapered axisymmetric fibres with a precalculated transverse mode structure. It deals with the fundamental mode electric field linearly polarised across the fibre axis. Its Fourier transform can be represented as [9, 24]

$$\overline{E}_\omega = \overline{G}(z,\omega)F(z,r,\omega)\exp[i\beta(z,\omega)z], \tag{1}$$

where z is the distance along the fibre; ω is the angular frequency; r is the radial coordinate; F is the transverse fundamental mode field distribution; and β is the propagation constant of the fundamental mode. With $G(z,\omega) = \overline{G}(z,\omega)\exp[i\beta(z,\omega)z]$, the one-way equation can be written in the form [9, 24]

$$\frac{\partial G(z,\omega)}{\partial z} - i\beta(z,\omega)G(z,\omega) + \alpha(\omega)G(z,\omega)$$

$$= \frac{2\pi i\omega^2\chi^{(3)}}{c^2\beta}\int_{-\infty}^{\infty}\int_{-\infty}^{\infty} d\omega_1 d\omega_2 K(z,\omega,\omega_1,\omega_1+\omega_2-\omega,\omega_2)$$

$$\times b(\omega-\omega_1)G(z,\omega_1)G^*(z,\omega_1+\omega_2-\omega)G(z,\omega), \tag{2}$$

where $\chi^{(3)}$ is the third-order nonlinear susceptibility; c is the speed of light in vacuum; the $b(\omega)$ function includes the instantaneous Kerr contribution and delayed Raman contribution; $\alpha(\omega)$ is the optical loss; and the function $K(z,\omega,\omega_1,\omega_1+\omega_2-\omega,\omega_2)$ is defined as

$$K(z,\omega,\omega_1,\omega_1+\omega_2-\omega,\omega_2)$$

$$= \int_0^\infty dr F(z,r,\omega_1)F^*(z,r,\omega_1+\omega_2-\omega)F(z,r,\omega_2)F^*(z,r,\omega). \tag{3}$$

To find the propagation constants and transverse electric field structures of the fundamental modes of axisymmetric germanate fibres of various diameters, we solved the problem of eigenvalues and eigenfunctions of the Helmholtz equation, which was represented mathematically as follows [25]:

$$\frac{d^2F}{dr^2} + \frac{1}{r}\frac{dF}{dr} + n^2(r,\omega)\frac{\omega^2}{c^2}F - \beta^2F = 0, \tag{4}$$

$$F(r\to\infty)\to 0, \tag{5}$$

$$\frac{dF}{dr}(r=0) = 0. \tag{6}$$

The normalisation of the function $F(r,\omega)$ has the form

$$\int_0^\infty |F(z,r,\omega)|^2 2\pi r dr = 1. \tag{7}$$

In our calculations, we assumed that the fibre had a silica cladding and that its core had a super-Gaussian GeO_2 dopant profile. The refractive index n as a function of wavelength λ was determined according to the following model:

$$n^2 = 1 + \sum_1^3 \frac{[SA_i + X_{GeO_2}(GA_i - SA_i)]\lambda^2}{\lambda^2 - [Sl_i + X_{GeO_2}(Gl_i - Sl_i)]^2}, \tag{8}$$

where $X_{GeO_2} = \exp(-r^4/r_0^4)$ is the germanium dioxide molar concentration distribution; r_0 is a characteristic core size; SA_i and Sl_i are the Sellmeier coefficients for silica; and GA_i and Gl_i are those for germanium dioxide [26] (SA_1 = 0.6961663, Sl_1 = 0.0684043, SA_2 = 0.4079426, Sl_2 = 0.1162414, SA_3 = 0.8974794, Sl_3 = 9.896161, GA_1 = 0.80686642, Gl_1 = 0.068972606, GA_2 = 0.71815848, Gl_2 = 0.15396605, GA_3 = 0.85416831, Gl_3 = 11.841931).

Outside the fibre core, the electric field of the transverse modes falls off almost exponentially at high r values [25], so the finite dimensions of the silica cladding can be neglected and the cladding can be taken to be infinite in calculations. The eigenvalues and eigenfunctions of the Helmholtz equation were found using a finite-difference scheme. We changed the variable $r = r_y y/(1-y)$, where r_y is a characteristic size related to the core diameter. This substitution allowed us to transform the infinite interval $0 \leqslant r < \infty$ to the finite one $0 \leqslant y < 1$.

Losses in fibres are a rather important characteristic because they can limit optical pulse frequency conversion at wavelengths above 2 μm. It is known that, in addition to the fundamental losses associated with Rayleigh scattering and absorption in the electron and phonon subsystems, there are high excess (anomalous) losses at the core–cladding interface [27–30]. In our calculations, we introduced a model loss function using previous experimental data [27, 31]. Namely, we assumed that

$$\alpha = A_{UV}\exp(\lambda_{UV}/\lambda) + A_{IR}\exp(-\lambda_{IR}/\lambda), \tag{9}$$

where $A_{IR} = 10^{-3}$ dB km^{-1}, $A_{UV} = 10^9$ dB km^{-1}, $\lambda_{UV} = 4.67$ μm and $\lambda_{IR} = 47.8$ μm.

An important parameter of fibres is their cubic nonlinearity coefficient, proportional to the nonlinear contribution of n_2 to the refractive index [22]. It is worth pointing out that the n_2 values reported for germanium dioxide in the literature differ rather markedly. In particular, Rottwitt and Povlsen [32] reported $n_2 = 12.5\times10^{-20}$ m^2 W^{-1}, whereas Yatsenko and Mavritsky [33], who measured the nonlinear refractive index of germanate fibres with a core containing 97 mol % GeO_2, obtained $n_2 = 5\times10^{-20}$ m^2 W^{-1}. The latter value was used in our theoretical analysis.

In taking into account the contribution of stimulated Raman scattering, the model response function $R(t)$ of germanate glass was assumed to be similar to that of silica glass [22]:

$$R(t) = (1-f_R)\delta(t) + f_R\Theta h_R(t),$$

$$h_R(t) = \frac{\tau_1^2+\tau_2^2}{\tau_1\tau_2^2}\exp(-t/\tau_2)\sin(t/\tau_1), \tag{10}$$

where f_R is the partial contribution of the Raman response; $\delta(t)$ is the delta function; $\Theta(t)$ is the Heaviside step function; and τ_1 and τ_2 are the characteristic Raman response times. However, f_R, τ_1 and τ_2 were calculated from the experimentally measured Raman gain spectrum $g_R(\omega)$ [34], related to the response function by [22]

$$g_R(\omega) = \frac{\omega_0}{cn_0} f_R \chi^{(3)} \mathrm{Im}[h_R(\omega)], \quad (11)$$

where n_0 is the refractive index at the centre frequency ω_0. We obtained $f_R = 0.25$, $\tau_1 = 13$ fs and $\tau_2 = 90$ fs, and used these values in our calculations. Note that Rottwitt and Povlsen [32] reported the following parameters: $f_R = 0.13$, $\tau_1 = 12$ fs and $\tau_2 = 83$ fs. The considerable discrepancy between the f_R values obtained in this study and in Ref. [32] is attributable to the fact that different n_2 values were used.

In mathematical modelling of ultrashort pulse propagation in tapered fibres with group velocity dispersion varying along their length, we used the pseudospectral, split-step Fourier method (SSFM) and fast Fourier transformation [22]. Note that the above single-mode model was used previously to analyse ultrashort pulse propagation in germanate fibres of constant diameter and made it possible to obtain interesting results, supported by experimental data, including those on the generation of supercontinuum and tunable ultrashort pulses at wavelengths of up to 3 μm [9, 10].

Figure 1 shows the calculated group velocity dispersion and nonlinearity coefficients of fibres with a super-Gaussian doping profile of their core, whose diameter (full width at half maximum of the refractive index profile) is varied from 2 to 4 μm in 0.1-μm steps (as a result, the cutoff wavelength varies from 1.7 to 3.5 μm). In the case of the thicker fibres, the contribution of the waveguide component is relatively small and the zero dispersion wavelength is about 1.5 μm, being close to the zero material dispersion point. With decreasing core diameter, the zero dispersion point shifts to longer wavelengths. At wavelengths near 1.5 μm, the fundamental mode field is well-localised near the fibre core, the effective mode size is small, and, accordingly, the nonlinearity coefficient is large. With increasing wavelength, the mode size increases and the nonlinearity coefficient drops.

Such fibres with constant diameter d can be used for supercontinuum generation and soliton pulse wavelength conversion to above 2 μm owing to stimulated Raman scattering, which leads to the amplification of low-frequency pulse components at the expense of high-frequency components and, hence, to a gradual decrease in the signal's carrier frequency. In the adiabatic approximation, the Raman shift rate of a soliton's carrier frequency Ω can be evaluated as [11]

$$\frac{d\Omega}{dz} = -\frac{[\gamma(\Omega)]^4 T_R W^4}{30|\beta_2(\Omega)|^3}, \quad (12)$$

where γ is the nonlinearity coefficient; $\beta_2 = \partial^2\beta/\partial\omega^2$ is the group velocity dispersion; W is the soliton energy; and T_R is the characteristic Raman response time [22]. It follows from (12) that the greater the decrease in carrier frequency, the slower the shift rate, because the functions $[\gamma(\Omega)]^4$ and $1/|\beta_2(\Omega)|^3$ drop very sharply with decreasing Ω and the $W(\Omega)$ energy decreases along the soliton trajectory. In view of this, we propose that the tapered fibre diameter should be adiabatically (gradually) reduced so that, at the centre frequency of the soliton, the parameter $\gamma^4/|\beta_2|^3$ remains almost constant, i.e. the Raman shift rate far exceeds that in a constant core diameter fibre.

Since with decreasing fibre diameter the zero dispersion wavelength varies first more slowly than when the minimum diameter is approached, the $d(z)$ profile can be chosen so that the derivative of this function decreases in magnitude with increasing z. The model profile chosen is shown in Fig. 2.

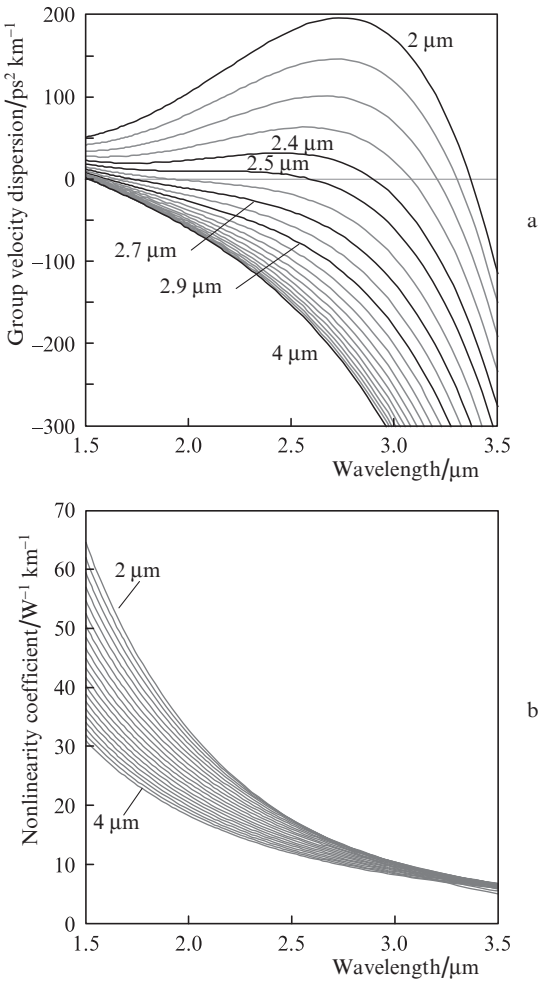

Figure 1. Calculated (a) group velocity dispersion and (b) nonlinearity coefficients of germanate fibres with core diameters from 2 to 4 μm. Neighbouring curves differ in core diameter by 0.1 μm.

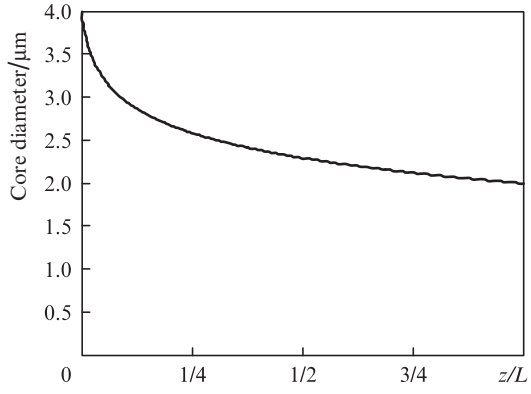

Figure 2. Core diameter vs. z-coordinate along the axis of germanate DDF of length L.

In numerical modelling using Eqn (2), the input pulse was sech-shaped at a centre wavelength of 2 μm and had an energy $W_0 = 2$ nJ and duration $T_{0.5} = 100$ fs (full width at half-maximum intensity). Such a signal can readily be obtained using a hybrid erbium/thulium fibre laser system [35]. The electric field of the pulse can be represented as $E(0,t) = \sqrt{W_0/(2T_0)} \times \exp(-i\omega_0 t)/\cosh(t/T_0)$, where $T_0 = T_{0.5}/[2\ln(1+2^{1/2})]$. The soli-

ton order for such a pulse launched into fibre with a core diameter of 4 μm can be estimated as $N = [\gamma W_0 T_0/(2|\beta_2|)]^{1/2} \approx 4$, so the initial stage in the spectral–temporal evolution of the pulse is determined by high-order soliton dynamics [22]. Self-phase modulation leads to broadening of the spectrum, accompanied by time-domain narrowing of the pulse due to the anomalous dispersion. The result is the formation of a narrow, strong peak on top of a broad pedestal. After the maximum compression point, the pulse breaks up into solitons in the anomalous dispersion region and dispersive waves in the normal dispersion region [22].

We followed the evolution of the longest wavelength soliton and attempted to increase its wavelength to above 3 μm. Figure 3 illustrates the spectral evolution of a pulse along the z-coordinate of a DDF of length $L = 80$ cm. Also represented for comparison is the evolution of identical pulses in fibres with constant diameters throughout their length. At core diameters of 4, 2.9 and 2.7 μm, the pulse is located in the anomalous dispersion region and its subsequent nonlinear dynamics are determined by high-order solitons. At core diameters of 2.5 and 2.4 μm, the pulse propagates in the normal dispersion region, so its nonlinear dynamics have qualitative distinctions. Self-phase modulation causes broadening of the spectrum, but the normal dispersion leads not to compression but to stretching of the signal. If passing through the zero dispersion point (at $d = 2.5$ μm), the pulse breaks up into individual spectral components. It should be emphasised however that a spectrally isolated signal having a wavelength of 3 μm and formed over a length $z \approx 30$ cm has a non-soliton nature and its wavelength remains essentially constant with increasing z. At $d = 2.4$ μm, the broadened spectrum does not reach the zero dispersion point, and the pulse does not break up into separate parts in time domain but only becomes longer throughout its path.

Figure 3 demonstrates that the maximum frequency shift takes place in the DDF. The centre wavelength of the corresponding soliton is 3.4 μm, and its spectrum contains components up to 3.5 μm. At core diameters of 4, 2.9 and 2.7 μm, the Raman shift rate considerably decreases with increasing z because of the sharp drop in $\gamma^4/|\beta_2|^3$ at the centre frequency of the soliton, whereas the shift rate in the DDF is rather high throughout the propagation path. Figure 4 shows the centre wavelength as a function of z for the longest wavelength Raman soliton. The dashed lines represent initial portions where there is no fundamental soliton.

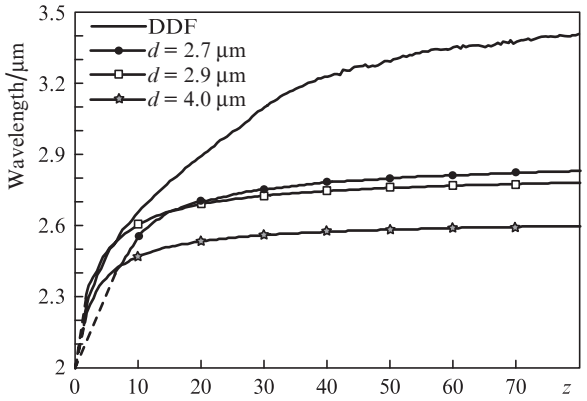

Figure 4. Centre wavelength vs. z-coordinate for the longest wavelength Raman soliton in DDF and fibres with a constant core diameter d.

It is reasonable to choose a relatively large core diameter at the DDF input to ensure that, during the development of high-order soliton dynamics, the first soliton formed had sufficiently high energy. In particular, at an input core diameter $d = 4$ μm the energy of a soliton formed near $z = 3$ cm is about 1 nJ, but at the output it is a factor of 2 lower, 0.5 nJ, because of the loss represented by Eqn (9) and the Raman loss associated with molecular vibrations. It is known that the Raman

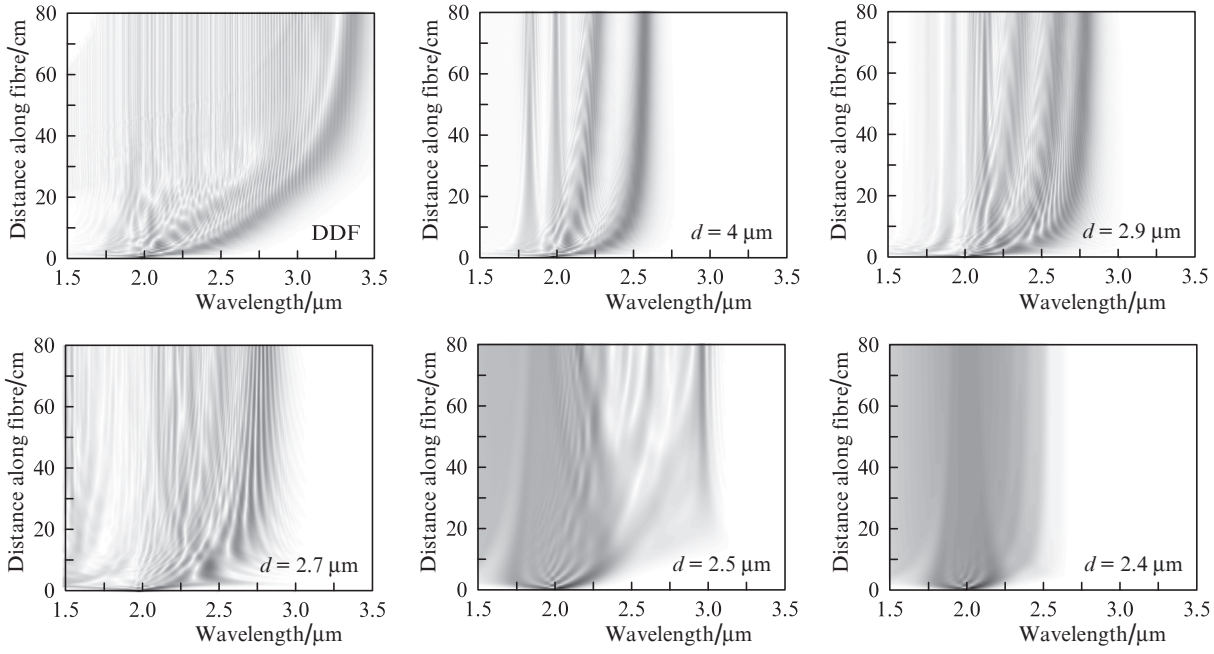

Figure 3. Spectral evolution of sech-shaped pulses of 2-nJ energy and 100-fs duration in DDF and fibres with a constant core diameter d.

loss can be evaluated from the constraint W/Ω = const for a soliton at $\alpha = 0$ [36]. At smaller core diameters, the soliton order at the input increases because of the decrease in $|\beta_2|$ and increase in γ, and the fraction of energy in the first soliton drops. There is some optimal input core diameter. It is seen in Fig. 1a that, at a large increase in diameter, the dispersion curve shifts very little. However, at a large diameter d, LP_{11}, LP_{21}, LP_{02} and other higher modes can be effectively excited in the fibre, which will be a parasitic effect, because it will be accompanied by a reduction in the energy of the fundamental mode LP_{01} and, accordingly, in the Raman shift rate, given by Eqn (12). The diameter of the output tapered fibre end determines the extreme position of the zero dispersion point. However, at very small d the zero dispersion point shifts very little. In our case, the optimal change in d is by a factor of 2: from 4 to 2 μm. In the adiabatic approximation, the maximum Raman soliton wavelength can be estimated merely as the maximum zero dispersion wavelength because, at small core diameters, the dispersion curve falls off very sharply after the zero point. In the case of DDF with large L, adiabaticity may be violated because of the $\alpha(\Omega)$ loss, the pulse may stop being a soliton at some instant in time and leave the anomalous dispersion region, and the zero point may 'leap' over the carrier frequency Ω. Too small lengths are also nonoptimal because they violate adiabaticity and the pulse has no time to 'adjust' its parameters to those of a soliton. In particular, the characteristic nonlinear length of a Raman soliton can be estimated at $L_{NL} = 2T_0/(\gamma W) \approx 0.5$ cm for soliton wavelengths near 2.5 μm and at $L_{NL} \approx 1$ cm for wavelengths above 3 μm, so the characteristic length scale for variations in the parameters of the DDF should exceed L_{NL}.

3. Conclusions

Tapered germanate fibres with group velocity dispersion varying along their length have been proposed for effective conversion of ultrashort nanojoule pulses generated by a fibre laser system at 2 μm to the mid-IR region. Using a one-way wave equation that takes into account nonlinear and dispersion effects and optical losses, we have shown that, in fibres with anomalous dispersion decreasing along their length, wavelengths of up to 3.5 μm can be reached, which are unattainable in the case of fibres with a constant core diameter at the same input signal parameters. Effective conversion is due to the Raman soliton self-frequency shift. The parameters of the tapered fibre are varied so that the Raman shift rate remains sufficiently high throughout the propagation path. The characteristic fibre length is then of the order of 1 m and the input core diameter is twice the output diameter. In the adiabatic approximation, the maximum attainable wavelength is determined by the zero dispersion wavelength of the fibre near its output end. The present results can be useful in designing a mid-IR all-fibre laser source using standard components and fibre-optic technologies.

Acknowledgements. This research was supported by the Russian Foundation for Basic Research (Grant Nos 14-02-00537 a, 14-22-02076 ofi_m and 15-32-20641 mol_a_ved) and the Presidium of the Russian Academy of Sciences (Extreme Light Fields and Their Applications Programme).

References

1. Andriukaitis G., Balčiūnas T., Ališauskas S., Pugžlys A., Baltuška A., Popmintchev T., Chen M.-C., Murnane M.M., Kapteyn H.C. *Opt. Lett.*, **36**, 2755 (2011).
2. Zheltikov A.M., Voronin A.A., Kienberger R., Krausz F., Korn G. *Phys. Rev. Lett.*, **105**, 103901 (2010).
3. Sorokina I.T., Dvoyrin V.V., Tolstik N., Sorokin E. *IEEE J. Sel. Top. Quantum Electron.*, **20**, 0903412 (2014).
4. Xia C.A., Kumar M., Kulkarni O.P., Islam M.N., Terry F.L. Jr., Freeman M.J., Poulain M., Maze G. *Opt. Express*, **31**, 2553 (2006).
5. Lægsgaard J., Tu H. *Opt. Lett.*, **38**, 4518 (2013).
6. Kamynin V.A., Kurkov A.S., Mashinsky V.M. *Laser Phys. Lett.*, **9**, 219 (2012).
7. Anashkina E.A., Andrianov A.V., Koptev M.Yu., Mashinsky V.M., Muraviov S.V., Kim A.V. *Opt. Express*, **20**, 27102 (2012).
8. Zhang M., Kelleher E.J.R., Runcorn T.H., Mashinsky V.M., Medvedkov O.I., Dianov E.M., Popa D., Milana S., Hasan T., Sun Z., Bonaccorso F., Jiang Z., Flahaut E., Chapman B.H., Ferrari A.C., Popov S.V., Taylor J.R. *Opt. Express*, **21**, 23261 (2013).
9. Anashkina E.A., Andrianov A.V., Koptev M.Yu., Muravyev S.V., Kim A.V. *IEEE J. Sel. Top. Quantum Electron.*, **20**, 643 (2014).
10. Anashkina E.A., Andrianov A.V., Koptev M.Yu., Muravyev S.V., Kim A.V. *Opt. Lett.*, **39**, 2963 (2014).
11. Kivshar Y.S., Agrawal G.P. *Optical Solitons: From Fibers to Photonic Crystals* (New York: Acad. Press, 2003).
12. Chernikov S.V., Richardson D.J., Payne D.N., Dianov E.M. *Opt. Lett.*, **18**, 476 (1993).
13. Shumin Z., Fuyun L., Wencheng X., Shiping Y., Jian W., Xiaoyi D. *Opt. Commun.*, **237**, 1 (2004).
14. Turitsyn S.K., Fedoruk M.P., Gornakova A. *Opt. Lett.*, **24**, 869 (1999).
15. Aseeva N.V., Gromov E.M., Tyutin V.V. *Chaos*, **23**, 013143 (2013).
16. Gromov E.M., Malomed B.A. *Opt. Commun.*, **320**, 88 (2014).
17. Zheltikov A.M. *J. Opt. Soc. Am. B*, **26**, 946 (2009).
18. Chan M.-C., Chia S.-H., Liu T.-M., Tsai T.-H., Ho M.-C., Ivanov A.A., Zheltikov A.M., Liu J.-Y., Liu H.-L., Sun S.-K. *IEEE Photonics Technol. Lett.*, **20**, 900 (2008).
19. Andrianov A.V., Muravyev S.V., Kim A.V., Sysolyatin A.A. *Pis'ma Zh. Eksp. Teor. Fiz.*, **85**, 446 (2007) [*JETP Lett.*, **85**, 364 (2007)].
20. Andrianov A., Kim A., Muraviov S., Sysoliatin A. *Opt. Lett.*, **34**, 3193 (2009).
21. Bogatyrev V.A., Bubnov M.M., Dianov E.M., Kurkov A.S., Mamyshev P.V., Prokhorov A.M., Rumyantsev S.D., Semenov V.A., Semenov S.L., Sysoliatin A.A., Chernikov S.V., Gur'yanov A.N., Devyatykh G.G., Miroshnichenko S.I. *J. Lightwave Technol.*, **9**, 561 (1991).
22. Agrawal G.P. *Nonlinear Fiber Optics* (London: Elsevier, 2013).
23. Brabec T., Krausz F. *Phys. Rev. Lett.*, **78**, 3282 (1997).
24. Laegsgaard J. *Opt. Express*, **15**, 16110 (2007).
25. Snyder A.W., Love J.D. *Optical Waveguide Theory* (London: Chapman and Hall, 1983; Moscow: Radio i Svyaz', 1987).
26. Fleming J.W. *Appl. Opt.*, **23**, 4486 (1984).
27. Dianov E.M., Mashinsky V.M. *J. Lightwave Technol.*, **23**, 3500 (2005).
28. Lines M.E., Reed W.A., Di Giovanni D.J., Hamblin J.R. *Electron. Lett.*, **35**, 1009 (1999).
29. Likhachev M.E., Bubnov M.M., Semjonov S.L., Khopin V.F., Salganskii M.Yu., Gur'yanov A.N., Dianov E.M. *Kvantovaya Elektron.*, **34**, 241 (2004) [*Quantum Electron.*, **34**, 241 (2004)].

30. Bubnov M.M., Semjonov S.L., Likhachev M.E., Dianov E.M., Khopin V.F., Salganskii M.Yu., Guryanov A.N., Fajardo J.C., Kuksenkov D.V., Koh J., Mazumder P. *IEEE Photonics Technol. Lett.*, **16**, 1870 (2004).
31. Mashinsky V.M., Neustruev V.B., Dvoyrin V.V., Vasiliev S.A., Medvedkov O.I., Bufetov I.A., Shubin A.V., Dianov E.M., Guryanov A.N., Khopin V.F., Salgansky M.Yu. *Opt. Lett.*, **29**, 2596 (2004).
32. Rottwitt K., Povlsen J.H. *J. Lightwave Technol.*, **23**, 3597 (2005).
33. Yatsenko Y., Mavritsky A. *Opt. Lett.*, **32**, 3257 (2007).
34. Galeener F., Millelsen J., Geils R., Mosby W. *Appl. Phys. Lett.*, **32**, 34 (1978).
35. Koptev M.Yu., Anashkina E.A., Andrianov A.V., Muravyev S.V., Kim A.V. *Opt. Lett.*, **39**, 2008 (2014).
36. Mamyshev P., Chernikov S. *Opt. Lett.*, **15**, 1076 (1990).